Title: Ear wound healing in MRL/MpJ mice is associated with gut microbiome composition and is transferable to non-healer mice via microbiome transplantation

Author Block:

Cassandra Velasco[2]

Christopher Dunn[2]

Cassandra Sturdy[1]

Vladislav Izda[1]

Jake Martin[1]

Alexander Rivas[3]

Jeffrey McNaughton[2]

Matlock A. Jeffries[1,2] (ORCID ID: 0000-0001-9516-4312)

1. Oklahoma Medical Research Foundation, Arthritis & Clinical Immunology Program, Oklahoma City, OK
2. University of Oklahoma Health Sciences Center, Department of Internal Medicine, Division of Rheumatology, Immunology, and Allergy, Oklahoma City, OK
3. University of Arkansas for Medical Sciences, Little Rock, AR

Contact information for correspondence:

Matlock A. Jeffries, MD
Oklahoma Medical Research Foundation
825 NE 13th Street, Laboratory MC400
Oklahoma City, OK 73104
Phone: (405) 271-7438
Fax: (888) 319-1241
Email: matlock-jeffries@omrf.org

Acknowledgments and Affiliations:

This work was supported by NIH grants K08AR070891, P20GM125528, R61AR078075, and R01AR076440, along with the Congressionally Directed Medical Research Program grant PR191652. The content is solely the responsibility of the authors and does not necessarily represent the official views of the National Institutes of Health. The funding source had no involvement in the writing of this article.

This work was supported by a Physician Scientist Development Award (PDSA) from the Presbyterian Health Foundation and an Oklahoma Center for the Advancement of Science and Technology (OCAST) Oklahoma Health Research Grant.

COI: The authors declare no conflicts of interest.

Abstract:

Objective: Adult cartilage has limited repair capacity. MRL/MpJ mice, by contrast, are capable of spontaneously healing ear punctures. This study was undertaken to characterize microbiome differences between healer and nonhealer mice and to evaluate microbiome transplantation as a novel regenerative therapy.

Methods: We transplanted C57BL/6J mice with MRL/MpJ cecal contents in mice at weaning and as adults (n=57) and measured earhole closure 4 weeks after a 2.0mm punch and compared to vehicle-transplanted MRL and B6 (n=25) and B6-transplanted MRL (n=20) mice. Sex effects, timing of transplant relative to earpunch, and transgenerational heritability were evaluated. In a subset (n=58), cecal microbiomes were profiled by 16S sequencing and compared to earhole closure rates. Microbial metagenomes were imputed using PICRUSt.

Results: Transplantation of B6 mice with MRL microbiota, either in weanlings or adults, improved earhole closure rates. Transplantation prior to ear punch was associated with the greatest earhole closure. Offspring of transplanted mice healed better than controls. Several microbiome clades were correlated with healing, including Firmicutes, Lactobacillales, and Verrucomicrobia. Gram-negative organisms were reduced. Females of all groups tended to heal better than males, female microbiota resembled MRL mice.

Conclusion: In this study, we found an association between the microbiome and tissue regeneration in MRL mice and demonstrate that this trait can be transferred to nonhealer mice via microbiome transplantation. We identified several microbiome clades associated

66 with healing. Future studies should evaluate the mechanisms underlying these findings
67 and confirm our results in murine OA.

68 **Introduction**

69

70 The Murphy Roths Large (MRL) mouse strain was originally selected for large body size
71 in the 1960s; at the F_{12} generation, these mice developed a spontaneous mutation in the
72 immune regulator *Fas*. This MRL/*lpr* variant is commonly used as a lupus mouse model
73 [1,2], whereas the non-*Fas*-mutant MRL/MpJ strain are generally used as a control in
74 autoimmune disease experiments. In 1998, MRL/MpJ mice were unexpectedly found to
75 fully close 2.0mm earhole puncture wounds after 4 weeks [3,4], subsequent studies have
76 shown a generalized healing phenotype in MRL mice, including neonatal digital tip
77 regrowth [5,6], peripheral nerve regeneration [7], and cardiac wound healing [8,9].

78

79 Approximately 75% of the MRL genome is derived from the LG/J parent strain. In
80 experiments over the past decade, several backcrosses of LG/J and SM/J (a nonhealer
81 strain) have been generated to evaluate the heritability of earhole closure and OA
82 protection. Those backcrosses most genetically similar to LG/J mice have the greatest
83 regenerative earhole wound healing capacity [10], as well as the highest articular cartilage
84 regeneration ability [11,12]. Genetic analyses of these strains have been conducted [13–
85 16], with several genes and gene pathways now known to be involved with wound healing
86 [17], including DNA repair and Wnt signaling [16]. However, a 2015 report made an
87 unexpected discovery: C57BL/6J mice did not improve either ear-wound or articular
88 cartilage healing following an allogeneic bone marrow transplant from MRL/MpJ donors
89 [18], and a recent study found the heritability of OA protection in LG/SM backcrosses to

be only moderate (0.18 to 0.58) [19], suggesting that other environmental factors play a role in MRL healing.

Of particular human relevance, MRL mice also regenerate knee cartilage following full-thickness cartilage injury [20], protecting them against the development of osteoarthritis (OA) Further studies have demonstrated a strong correlation between this articular cartilage healing phenotype and healing of ear puncture holes [11]. OA is a chronic musculoskeletal disease characterized by pain and progressive loss of joint function leading to reduced mobility and is associated with a variety of comorbidities including heart disease, stroke, metabolic syndrome, and anxiety/depression [21–23]. It is the most common musculoskeletal disease worldwide and is the leading cause of chronic disability in the US, affecting roughly half of adults over 65 years of age [24]. There are no disease modifying drugs approved for OA; therefore, much attention has recently been focused on the development of novel regenerative strategies to treat this devastating disease.

In the present study, we set out to investigate whether the gut microbiome is associated with the cartilage healing phenotype observed in MRL mice generally, whether this trait is transferable to nonhealer mice via alteration of the gut microbiome, and whether microbiome differences are associated with sex-associated discordant ear hole closure rates in MRL mice.

Methods

113 *Ethics Statement:*

114 The institutional review board and institutional animal care and use committees of all
115 involved institutions approved this study; a detailed protocol was developed prior to
116 beginning this study; this protocol and subsequent addenda were reviewed by the animal
117 care and use committee of all involved institutions.

118

119 *Mouse husbandry:*

120 Young male and female (4 week-old) C57BL6/J or MRL/MpJ mice were purchased from
121 Jackson Laboratories (Bar Harbor, ME, USA) and housed at the Oklahoma Medical
122 Research Foundation (OMRF). Breeding pairs were created and pups were used for
123 some experiments. All animals were permitted ad libitum access to food and water
124 (NIH31). The OMRF animal facility uses a 12-hour light-dark cycle. All animal husbandry
125 procedures adhered to the NIH Guide for the Care and Use of Laboratory Animals. There
126 were no adverse events (expected or unexpected) during the course of this experiment.

127

128 *Mouse cecal microbiota transplantation procedure:*

129 Cecal donor mice (B6 or MRL, 10-14 weeks of age) were sacrificed and immediately
130 dissected under sterile conditions. The cecum was removed and cecal contents
131 transferred to a sterile tube containing a 1:1 mixture of glycerol and phosphate-buffered
132 saline (5mL), which was then filtered through a 100μM filter. The resulting mixture was
133 aliquoted and frozen at -80C for subsequent transplantation. At 3-4 weeks of age,
134 recipient mice were pretreated with omeprazole (50mg/kg body weight) as previously
135 described [25,26]. Omeprazole was then sequentially administered via oral gavage

136 once daily for 3 days prior to microbiome transfer. On the day of cecal transplantation,
137 100uL of transplant material (per 3-4-week-old recipient mouse) or 300uL of transplant
138 material (per 16-week-old adult mouse) was transplanted via oral gavage using flexible
139 30mm polypropylene tubes (Instech, Plymouth Meeting, PA, USA). Mice were then
140 moved to clean cages and segregated by transplant group. For adult transplantation
141 experiments, 12 week-old mice were given 50mg/kg omeprazole once daily for 3 days,
142 then transplanted on day 4, as above.
143
144 *Mouse earhole puncture, sacrifice procedures:*
145 At 6 weeks of age (for young animals) or 18 weeks of age (for adult animals), mice were
146 ear punched using a 2mm through-and-through ear punch. Mice were sacrificed 4 weeks
147 after ear punch (10 weeks of age for young and 22 weeks of age for adult animals). Whole
148 blood was collected via cardiac puncture, allowed to clot for at least 30 minutes, then
149 centrifuged and serum removed for subsequent analysis. Final earhole size was
150 measured using digital calipers, investigators were blinded to mouse group during earhole
151 size measurements. Cecal material was collected immediately after sacrificing animals
152 and flash frozen in liquid nitrogen. Cecal DNA was extracted using a QIAamp DNA
153 microbiome kit (Qiagen).
154
155 *16S ribosomal RNA (rRNA) gene sequencing:*
156 Microbial profiles were determined by sequencing a ~460bp region including the V3 and
157 V4 variable region of bacterial 16S rRNA genes. The gene fragment was amplified from
158 approximately 30ng of DNA in each sample (primers in Supplementary Table 1) using a

159 high-fidelity polymerase (NEB Q5, New England Biolabs)[27] and confirmed by 1%
160 agarose gel electrophoresis. PCR master mixes were decontaminated with double-
161 stranded DNAse treatment (PCR decontamination kit, Arcticzymes, Tromsø, Norway).
162 Sterile water was processed using the same procedure as a negative control. Illumina
163 Nextera XT indices were attached (Illumina), pooled in equimolar amounts, and
164 sequenced on an Illumina miSeq sequencer using a 300bp paired-end sequencing
165 protocol by the Clinical Genomics Center at OMRF.
166
167 *16S rRNA OTU classification:*
168 Quality filtering, operational taxonomic unit (OTU) classification and microbial diversity
169 analysis were performed using the Quantitative Insights into Microbial Ecology (QIIME)
170 software package, version 1.9.1[28]. Sequences were assigned to OTUs using the
171 UCLUST algorithm[29] with a 97% pairwise identity threshold and taxonomy assigned
172 using the GreenGenes 13_8 database[30].
173
174 *Diversity analyses:*
175 Alpha diversity was characterized using the observed OTUs method following rarefaction
176 to the lowest number of OTUs present per group (123,543). Beta diversity was evaluated
177 on a variance-adjusted, weighted unifrac model. Principal component analysis was
178 performed and an Adonis (permuted analysis of variance, a multi-factor PERMANOVA)
179 test with 999 permutations was used to calculate the statistical significance of group
180 differences[31,32].
181

182 *Group analyses:*

183 Group analyses were performed using the linear discriminant analysis effect size (LEfSe)
184 pipeline[33]. LEfSe performs a non-parametric Kruskal-Wallis sum-rank test[34] to detect
185 features with significant differential abundance between groups, $P \leq 0.01$ was considered
186 significant. Next, it uses a linear discriminant analysis (LDA)[35] to estimate the effect
187 size of each differentially abundant feature. An LDA threshold of ≥2 was considered
188 significant[36]. QIIME was used to calculate group Benjamini-Hochberg FDR-corrected
189 q-values; $q \leq 0.01$ was chosen as the 'FDR-corrected' significance threshold. For Gram
190 status comparisons, differences were evaluated by Student t-tests, $P \leq 0.05$ was
191 considered statistically significant. Correlations were determined by comparing earhole
192 closure rates of individual animals with microbiome clades, $P \leq 0.05$ was considered
193 statistically significant. No samples were excluded from analysis.

194

195 *Prediction of metagenome content and imputed bacterial functional classification:*

196 The Phylogenetic Investigation of Communities by Reconstruction of Unobserved States
197 (PICRUSt) software package[37] was used to impute bacterial metagenomes from our
198 16S deep sequencing microbial DNA data, and functional annotation applied using the
199 Kyoto Encyclopedia of Gene and Genomes (KEGG) catalog[38]. Statistical analysis was
200 performed using the Statistical Analysis of Metagenomic Profiles (STAMP) package[39].
201 Statistical significance and effect sizes among the three groups (human OA-eroded, OA-
202 intact, and control) were calculated using ANOVA. Statistical significance was defined as
203 Benjamini-Hochberg FDR corrected $P \leq 0.01$.

204

205 **Results:**

206

207 *Improved earhole closure in non-healer B6 mice transplanted with healer MRL cecal*
208 *material*

209 Our final analysis included 131 mice from 6 independent experiments. These included 25
210 B6 vehicle-transplanted control mice, 57 MRL-transplanted B6 mice, 29 MRL vehicle-
211 transplanted control mice, and 20 B6-transplanted MRL mice. B6-vehicle mice healed
212 earhole punches poorly (0.25±0.03mm, earhole healing 4 weeks after a 2mm earhole
213 punch, mean±SEM), whereas MRL-vehicle mice healed well (1.4±0.1mm). MRL-
214 transplanted B6 mice healed roughly three times as well as B6-vehicle mice, and half as
215 well as MRL-vehicle mice (0.74±0.05mm, *P*=6.9E-10 vs. B6-vehicle, *P*=5.2E-12 vs. MRL-
216 vehicle, **Figure 1A**). Transplantation of MRL mice with B6 cecal material did not reduce
217 MRL healing (B6-transplanted MRL 1.3±0.1 vs. MRL-vehicle 1.4±0.1, p=0.36).

218

219 *Earhole closure outcomes depend on the timing of microbiome transplantation*

220 Next, we determined whether the timing of microbiome transplantation relative to ear
221 punch would alter this healing phenotype. We performed ear punches of 6 week-old male
222 B6 mice, similar to previous experiments, then performed an MRL cecal transplantation
223 at 48 hours, 1 week, and 2 weeks after ear punch. There was a graded reduction in ear
224 wound healing capacity in mice transplanted after ear punch (**Figure 1B)**; the 48 hour
225 post-ear punch group (n=8) demonstrated superior healing compared to B6-vehicle mice
226 (0.56±0.06mm vs. 0.25±0.03mm, P=2.4E-5, n=8), although there was a trend towards
227 worse healing than mice transplanted at weaning (P=0.11). In mice transplanted 1 week

228 after ear punch, there was a trend towards improved healing (0.35±0.05mm, P=0.11,
229 n=7). Healing was not improved compared to vehicle controls in mice transplanted 2
230 weeks after ear punch (0.26±0.05mm, P=0.93, n=6).
231
232 *Adult transplant recipients heal as well as weanling recipients*
233 Although previous studies have indicated that the gut microbiome is most plastic in mice
234 at weaning [40], the disease our laboratory studies (OA) is a disease of adulthood.
235 Therefore, to broaden the applicability of our findings, we evaluated whether
236 transplantation of mice as adults would still confer improvements in earhole closure. To
237 this end, we performed cecal transplantation of B6 mice with MRL donor material (n=7)
238 or vehicle (n=4), as previously described, in 12 week-old mice with earhole punch 3 days
239 later. No differences in earhole closure rate were seen in mice transplanted at weaning
240 compared to mice transplanted as adults (**Figure 1C**) (B6-vehicle weaning: 0.25±0.03mm
241 earhole closure vs. adult: 0.25±0.07, *P*=0.47; MRL-transplanted B6 weaning: 0.74±0.05
242 vs. 0.60±0.06, *P*=0.25).
243
244 *Disparate healing rates in mice raised in-house compared to mice sourced from a*
245 *commercial vendor*
246 Both the bacterial and viral components of the mouse gut microbiome are heavily
247 influenced by diet and other environmental factors; in fact, previous studies have noted
248 dramatic differences in the microbiome when comparing the same strain of mouse
249 obtained from different commercial vendors [41,42]. Roughly half of our mouse
250 experiments were conducted on mice raised in-house (originally from Jackson

251 laboratories, but bred for use at OMRF, including donors and recipient animals), with the
252 other half being purchased commercially from Jackson laboratories and immediately used
253 for transplantation experiments as both donors and recipients. We found variations
254 earhole closure rates with in-house reared mice demonstrating worse healing in the B6-
255 vehicle group (commercial vendor: 0.31±0.03mm earhole closure vs. in-house:
256 0.16±0.05, *P*=0.01) and improved healing in MRL-transplanted B6 (vendor: 0.57±0.04 vs.
257 0.86±0.07, *P*=0.0036), with a trend towards improved healing in MRL-vehicle mice
258 (vendor: 1.38±0.06 vs. 1.65±0.1, *P*=0.08) (**Figure 1D**).
259
260 *Transgenerational heritability of microbiome-mediated improvements in earhole closure*
261 We then evaluated the heritability of improved earhole closure following microbiome
262 transplantation. We transplanted mice at weaning, as previously discussed, then created
263 breeding pairs consisting of MRL-transplanted B6 male with MRL-transplanted B6 female,
264 B6-vehicle male with MRL-transplanted B6 female, and MRL-transplanted B6 male with
265 B6-vehicle female. The offspring of these breeding pairs were ear punched at 6 weeks of
266 age and earholes measured 4 weeks later to align with the timeline of our previous
267 transplantation-at-weaning experiments. We found offspring of transplanted mice healed
268 significantly better than non-transplanted control mice (0.63±0.03mm, mean±SEM vs.
269 0.25±0.03mm, n=39 offspring, P=4.6E-11); there was a trend toward slightly worsened
270 healing compared to primary MRL-transplanted B6 mice (0.63±0.03mm vs.
271 0.74±0.05mm, P=0.092) (**Table 1, Figure 1E**). There were no differences in healing
272 among offspring where both sire and dam were transplanted compared to sire-only or

273 dam-only-transplanted offspring (both transplanted: 0.65±0.02mm, n=4, vs. one
274 transplanted: 0.63±0.03, n=35, P=0.61).
275
276 *Durable gut microbiome alterations following microbiome transplantation, and*
277 *microbiome clade associations with earhole closure rates*
278 Next, we profiled the cecal microbiomes of 43 animals, including 8 B6-vehicle (4 male
279 and 4 female), 8 MRL-transplanted B6 (4 male and 4 female), 8 MRL-vehicle (4 male and
280 4 female), and 19 offspring of MRL-transplanted B6 mice (11 male and 8 female). All
281 samples demonstrated high 16S sequencing quality, with raw OTU counts per sample
282 ranging from 123,543 to 456,880. There were no statistically significant differences in raw
283 OTU counts among any group.
284
285 First, we analyzed alpha diversity, a measure of the overall number of bacterial clades
286 present per group, using the observed OTU method following rarefaction to the lowest
287 OTU count (**Figure 2A**). MRL-vehicle samples demonstrated significantly higher alpha
288 diversity than the other groups (MRL-vehicle 736±15 mean OTUs vs. B6-vehicle 603±30,
289 P=0.0014, MRL-vehicle vs. MRL-transplanted B6 636±32, P=0.013, MRL-vehicle vs.
290 offspring of MRL-transplanted B6 615±12, P=5.44E-6). There were no statistically
291 significant differences in alpha diversity among B6-vehicle, MRL-transplanted B6, and
292 offspring of MRL-transplanted B6 mice. Beta diversity, a measure of diversity in the
293 composition of groups, was then computed by the permanova method; we saw significant
294 differences (P<0.001) among all groups (**Figure 2B**).
295

296 We found numerous differences in cecal microbial clades when comparing mouse groups
297 (**Figure 2C**). In B6-vehicle vs. MRL-vehicle groups, 57 clades were significantly different
298 **(Supplemental Table 2)**, in B6-vehicle vs. MRL-transplanted B6 groups, 17 clades were
299 different **(Supplementary Table 3)**, in MRL-vehicle vs. B6-transplanted MRL groups, 239
300 clades were different **(Supplementary Table 4)**, and finally, comparing progeny of MRL-
301 transplanted B6 mice to B6-vehicle mice, we found 55 differences **(Supplementary Table**
302 **5)**. A number of clade differences were shared among the various groups; for example,
303 members of phylum *Verrucomicrobia*, particularly genus *Akkermansia*, were consistently
304 characteristic of B6 mice or mice transplanted with B6 cecal content (LDA-ES 4.46,
305 *P*=0.0008 in MRL-vehicle vs. B6-vehicle comparisons; LDA-ES 4.23 with *P*=0.0008 in
306 MRL-transplanted B6 vs. B6-vehicle comparisons, LDA-ES 3.84, *P*=0.04 in progeny vs.
307 B6-vehicle, and LDA-ES 4.37 with *P*=0.0008 in B6-transplanted MRL vs. MRL-vehicle
308 comparisons). Conversely, phylum *Firmicutes* was consistently associated with MRL or
309 MRL-transplanted animals (LDA-ES 4.71, *P*=7.8E-4 in MRL-vehicle vs. B6-vehicle; LDA-
310 ES 4.22, *P*=0.003 in progeny vs. B6-vehicle; LDA-ES 4.56, *P*=7.8E-4 in B6-transplanted
311 MRL vs. MRL-vehicle). Within phylum *Firmicutes*, members of order *Clostridiales* were
312 characteristic of MRL or MRL-transplanted animals (LDA-ES 4.32, *P*=7.8E-4 in MRL-
313 vehicle vs. B6-vehicle; LDA-ES 3.76, *P*=0.04; LDA-ES 4.42, *P*=7.8E-4 in B6-transplanted
314 MRL vs. MRL-vehicle), as were members of order *Lactobacillales* (LDA-ES 2.80, *P*=7.8E-
315 4 in MRL-vehicle vs. B6-vehicle; LDA-ES 3.89, *P*=0.002 in MRL-transplanted B6 vs. B6-
316 vehicle). Comparing B6-transplanted MRL to MRL-vehicle mice, we identified the transfer
317 of B6-associated clades into recipient animals, including members of phylum
318 *Verrucomicrobiae* (LDA-ES 4.40, *P*=7.8E-4), whereas MRL-vehicle animals were again

319 characterized by members of the phylum *Firmicutes* (LDA-ES 4.56, *P*=7.8E-4), among
320 others. We then correlated microbial clades to individual earhole closure rates. We found
321 44 clades highly correlated **(Figure 2D, Supplementary Table 6)**, including positive
322 correlations with phylum *Firmicutes* (R=0.76, *P*=5.8E-8), order *Clostridiales* (R=0.72,
323 P=7.5E-7), and order *Lactobacillales* (R=0.55, *P*=5.4E-4). Negative correlations with
324 earhole closure rates were seen among phylum *Verrucomicrobia*, specifically genus
325 *Akkermansia* (R=-0.71, *P*=1E-6) and order *Burkholderiales* (R=-0.58, *P*=1.7E-4).
326
327 We next examined the Gram status of cecal contents in the present experiment. We found
328 a decrease in Gram-negative constituent organisms in groups with improved ear healing
329 (B6-vehicle fraction cecal reads Gram-negative 0.39±0.02 vs. MRL-transplanted B6
330 0.23±0.03 vs. MRL-vehicle 0.06±0.01, B6-vehicle vs. MRL-vehicle *P*=3.6E-9, B6-vehicle
331 vs. MRL-transplanted B6 *P*=1.4E-5). However, offspring of MRL-transplanted B6 mice did
332 not demonstrate a significant shift in microbiome Gram status (Offspring: 0.37±0.03,
333 *P*=0.7 vs. B6-vehicle). Nonetheless, individual Gram-negative bacterial fraction was
334 negatively correlated with individual earhole closure rates (**Figure 2E**, R=-0.67, *P*=3.6E-
335 6).
336
337 *Sex disparities in earhole closure rates, and correlations with gut microbiome constituents*
338 Female mice are less affected by surgically induced OA than are male mice [43]. As our
339 study included both sexes, we evaluated sex-related differences in earhole closure in
340 control and transplanted mice, as well as any shared, sex-related microbiome differences
341 that might underlie earhole closure variations. Earhole closure rates in MRL-transplanted

342 B6 mice were not affected by the sex of the MRL donor mouse (*P*=0.61), nor were rates
343 in B6-transplanted MRL mice affected by the sex of the B6 donor mouse (*P*=0.33).
344 However, we did find variation in earhole closure rates depending on the sex of the
345 recipient mouse **(Figure 3A)**. Female B6-vehicle demonstrated a trend towards an
346 improved healing response (*P*=0.059), with a similar trend found in female MRL-
347 transplanted B6 mice (*P*=0.096). Differences were seen in both female B6-transplanted
348 MRL and female MRL-vehicle mice, where healing was significantly better than their male
349 counterparts (*P*=0.0015 and P=4.2E-6 for B6-transplanted MRL and MRL-vehicle mice
350 respectively). Furthermore, in heritability experiments, found a roughly one-third
351 improvement in healing among female offspring compared to male offspring (*P*=0.0038,
352 **Figure 3A**).
353
354 For cecal 16S analysis, we pooled microbiome data from B6-vehicle, MRL-vehicle, and
355 MRL-transplanted B6 animals and compared by sex. We first evaluated alpha diversity
356 using the observed OTU method following rarefaction, as previously described, and did
357 not find any sex-related differences (males: 646±13 vs. females: 632±21, *P* = 0.57). We
358 found differences in beta diversity by sex both within mouse transplant groups (all
359 *P*<0.001), and when all animals were considered together (*P*=0.012) (**Figure 3B**). We
360 then analyzed our 16S data by pooling all animals from the above groups and comparing
361 male to female animals. We found 18 clades which were different between the groups
362 **(Figure 3C)**; among these, many were shared with those clades identified as
363 differentiating MRL and B6 animals, above. These included phylum *Verrucomicrobia*

364 (increased in males, LDA-ES 3.88, *P* = 0.02) and order *Clostridiales* (increased in
365 females, LDA-ES 3.99, *P*=0.01) **(Supplementary Table 7)**.
366
367 *Imputed functional analysis of earhole closure-associated gut microbiome changes*
368 To offer insight into bacterial metabolomic and metagenomic changes associated with
369 transplantation, we next imputed cecal microbiome metagenomic function using the
370 Phylogenetic Investigation of Communities by Reconstruction of Unobserved States
371 (PICRUSt) analysis package (40). We compared MRL-transplanted B6 to B6-vehicle
372 groups and identified 218 Kyoto Encyclopedia of Gene and Genomes (KEGG) pathways
373 altered within gut microbiota (**Supplementary Table 8**) at an FDR threshold of *P*≤0.01.
374 Of these, 48 were highly correlated with earhole closure rates (*P*≤0.01) (**Table 2**). The
375 strongest positive correlations included D-arginine and D-ornithine metabolism (R=0.73,
376 *P*=0.007), flavone and flavonol biosynthesis (R=0.72, *P*=0.005), and mineral absorption
377 (R=0.66, *P*=0.003), whereas negative correlations included beta-lactam resistance (R=-
378 0.78, *P*=0.003), penicillin and cephalosporin biosynthesis (R=-0.78, *P*=6E-4),
379 glycosphingolipid biosynthesis (R=-0.75, *P*=6E-4), and lipopolysaccharide biosynthesis
380 (R=-0.73, *P*=5E-4), among others.
381
382 **Discussion:**
383
384 In this study, we provide the first evidence that the spontaneous earhole phenotype seen
385 in MRL/MpJ mice is associated with specific gut microbiome constituents and is
386 transferable to nonhealer B6 mice via gut microbiome transplantation. Furthermore, we

387 describe novel sex discrepancies in earhole closure rates in B6 and MRL mice, where
388 female animals demonstrate improved healing compared to males. We find that
389 transplant-associated improvements in earhole wound closure are time dependent, and
390 that the best outcomes are achieved if gut microbiome transplantation occurs before ear
391 wounding. Intriguingly, offspring of MRL-transplanted B6 mice also demonstrate
392 improved healing compared to non-transplanted controls, indicating transgenerational
393 heritability. In cecal microbiome 16S sequencing analysis, we identified a number of
394 clades that are associated, both positively and negatively, with ear wound healing,
395 including phylum *Firmicutes*, order *Clostridiales*, order *Lactobacillales*, and phylum
396 *Verrucomicrobia*. We also found a negative association between Gram-negative
397 organisms and ear wound healing despite an increase in serum LPS levels in both MRL
398 and MRL-transplanted B6 animals.
399
400 These data offer a counterpoint to the prevailing dogma that the superhealing
401 characteristics of MRL mice are purely genetic in origin, as we demonstrate that roughly
402 half of the MRL-associated wound healing capacity can be transferred to nonhealer mice
403 via a single gut microbiome transplantation. We did not see a reduction in ear wound
404 healing capability of MRL mice following transplantation of a B6 microbiome despite
405 confirming a reduction in key healing-associated gut microbiome clades in B6-
406 transplanted animals, suggesting the microbiome is not the sole determinant of earhole
407 closure. Furthermore, although we noted transgenerational heritability of both the earhole
408 closure phenotype and cecal microbiota clades of MRL-transplanted B6 mice, we saw a
409 trend towards reduction of earhole closure in offspring compared to primary transplanted

410 animals (*P*=0.09), as well as a reversion of Gram-negative gut constituents in offspring
411 towards a 'baseline' B6 phenotype, suggesting that both the transplant-associated
412 microbiome changes and cartilage healing phenotype may be lost over multiple
413 generations. This raises the intriguing possibility that the unique genetic makeup of MRL
414 mice is itself leading to alterations of the gut microbiome, perhaps through divergent
415 immune responses within the gut, which subsequently contributes to the earhole closure
416 phenotype.
417
418 We also unexpectedly identified differences between male and female animals in both
419 earhole closure rates and gut microbiome constituent organisms. Previous studies have
420 highlighted a reduction in OA histopathologic severity in female mice, in both young and
421 old animals [43,44]. Although not evaluated directly in the context of OA, sex-specific
422 differences in the gut microbiome have been described in association with known OA risk
423 factors, including high fat diet-induced obesity [45,46] and advanced age [47]. In the
424 present study, our 16S analysis identified 18 sex-associated microbiome clades; among
425 these, 7 overlapped with our MRL vs. B6 comparison. In every case, healing-associated
426 clades were enriched in females, whereas nonhealing-associated clades were enriched
427 in males. If our earhole closure phenotype indeed correlates with protection from OA in
428 transplanted animals (to be evaluated in future studies), microbiome differences might
429 offer a novel explanation for differences in sex-associated OA risk un mice. In this regard,
430 our confirmation that the gut microbiome-mediated earhole closure phenotype is stable
431 even when transplanting adult animals bodes well for future studies of murine OA
432 prevention.

433

434 Relatively few studies have rigorously evaluated the microbiome in the context of human
435 cartilage regeneration through studies on OA. The largest to date, published in 2019 by
436 Boer et al., found four bacterial clades associated with knee pain among 867 adults within
437 the Dutch Rotterdam (RSIII) and LifeLines-DEEP OA cohorts [48]. These included class
438 *Bacilli*, order *Lactobacillales*, family *Streptococcaceae*, and genus *Streptococcus.* In the
439 present study, we found members of order *Lactobacillales* within the gut are strongly
440 associated with ear wound healing in MRL-transplanted B6 mice, as well as one of the
441 clades transgenerationally inherited to progeny of MRL-transplanted B6 mice.
442 *Lactobacillus* has been shown to be depleted within the gut during mouse aging [49], a
443 known risk factor for OA development. These findings align with our previous work which
444 identified *Lactobacillales* DNA as characteristic of both disease-free human control and
445 OA-protected MRL cartilage [50]. Similarly, we found family *Clostridiaceae* within cecal
446 microbiota to be highly correlated with ear wound healing, and we previously identified
447 this clade as associated with disease-free human cartilage. Members of the order
448 *Burkholderiales* were strongly negatively correlated with earhole closure; this order was
449 associated with OA cartilage in our previous study. In 2019, Rios et al. published a report
450 of decreased OA severity in a rat model following supplementation of a high fat/high
451 sucrose diet with prebiotic fiber; in their model, fiber treatment increased *Bifidobacterium*
452 and *Roseburia* and decreased *Clostridium* and *Akkermansia* [51]. In our data,
453 *Akkermansia* (within phylum *Verrucomicrobia*) was associated with poor healing,
454 corroborating these findings.

455

456 The transgenerational heritability we identified in this study is interesting; previous reports
457 have identified transgenerational heritability of microbiome-mediated inflammatory
458 conditions [52], and a paper in 2020 demonstrated transgenerational heritability of weight
459 gain, metabolic imbalance, and injury-induced OA for at least 2 generations following
460 high-fat diet treatment in mice [53]. Unfortunately, this study did not evaluate the
461 microbiome as a potential mediator of these effects. A number of studies have proposed
462 an interaction between the gut microbiome and host epigenetic mechanisms in mediating
463 transgenerational effects [54,55]
464
465 Despite the associations we have described in this study, the key unanswered question
466 is the mechanism driving cecal microbiome-mediated ear wound healing, which will no
467 doubt require substantial future investigation to unravel. It is possible that alterations in
468 the gut microbiome, through transplantation, may have induced systemic alterations in
469 microbial metabolites and lead to a generalized pro-healing environment. Conversely, the
470 metabolites of certain gut organisms, particularly short-chain fatty acids (SCFA), can
471 promote intestinal repair and wound healing locally by inducing healing-associated gene
472 expression in epithelial cells [56]. Another possible explanation would be the alteration of
473 the cutaneous microbiome at the site of wounding, presumably via fecal-skin inoculation.
474 Previous studies have indicated that altered skin flora plays a role in impaired cutaneous
475 healing [57–59], principally related to biofilm formation at the wound site, with an
476 associated increase in inflammatory cytokine production, limiting healing capacity [60].
477

478 Although we did not evaluate microbial metabolites directly, we did gain insight into
479 metabolite alterations indirectly through our imputed functional metagenomic analysis.
480 We found a variety of imputed KEGG pathways associated with earhole closure, including
481 a few with previous links to tissue regeneration/healing and OA development. These
482 included an association with flavone biosynthesis, previously associated with promotion
483 of wound healing in rats [61] and suggested as an anti-inflammatory agent for use in OA
484 (by reduction in NF-KB and MAPK activation) [62]. We also saw an association with D-
485 arginine and D-ornithine metabolism, both enhancers of wound healing in mice [63,64];
486 intriguingly, there is some evidence that plasma arginine levels are reduced in knee OA
487 patients [65]. Additional associations of interest include fatty acid elongation; serum fatty
488 acid chain length is associated with symptomatic end-stage OA [66], and the bacterial
489 secretion system, which enables the export of bacterial proteases to the extracellular
490 environment in the context of chronic wound establishment [67].
491
492 Finally, our finding of differences in earhole closure rates of animals raised in-house vs.
493 those purchased from a commercial vendor and immediately used is in line with previous
494 reports of cecal microbiome changes associated with various animal vendors [41,42].
495 This observation also reinforces the potential for variation in microbiome-linked
496 phenotypic changes like earhole closure related to geographic location and diet;
497 researchers should keep this in mind when designing future microbiome-related
498 experiments.
499

500 Our study has several limitations. First, performed transplantation of animals with an
501 already-existing microbiota rather than colonizing germ-free animals. Although using non-
502 germ-free animals introduces the possibility of confounding results by variations in
503 transplant engraftment, it also makes our study more compelling from a potential human
504 therapeutic perspective. Another limitation is our lack of a definitive mechanistic
505 explanation for the healing that we describe, this will no doubt require an extensive
506 evaluation of several factors including local and systemic inflammatory responses,
507 previously associated with healing in MRL mice [68], and cell cycle/DNA damage
508 response, also associated with healing in MRL and $p21^{-/-}$ mice [69]. Nevertheless, we felt
509 that a timely publication of our observations was necessary to spur further research in
510 this area. Finally, we limited our study to one spontaneous healer strain (MRL) and
511 analyzed only young and young-adult mice; future analyses should include other strains
512 and expand to evaluate the transplant-associated healing potential, if any, in older mice.
513
514 In summary, herein we offer the first description of the gut microbiome-associated nature
515 of the earhole cartilage healing phenotype previously described in MRL/MpJ mice, and
516 demonstrate that this trait can be conferred to nonhealer mice via a gut microbiome
517 transplantation. We identified several clades within the gut microbiome that are strongly
518 associated (both positively and negatively) with earhole closure, and demonstrate that
519 transgenerational inheritance of transplanted gut microbiome constituents and
520 microbiome-mediate earhole closure occurs. Furthermore, we found evidence for sex-
521 specific effects of both earhole closure and gut microbiome trends, with female animals
522 healing better than males in a variety of contexts. Finally, we identified a number of

523 differences in imputed metagenomes among healing-associated microbiome clades.
524 Future work should focus on determining the mechanism underlying this microbiome-
525 associated healing phenotype and expanding this analysis to include other animals
526 identified as superhealers, including LG/J mice, *Acomys* mice, and perhaps invertebrate
527 healers. The potential for a gut microbiome-mediated healing response should also be
528 evaluated in the context of OA, which may offer a unique avenue for future therapeutic
529 development.
530
531
532
533

534 **Table 1: Earhole closure rates 4 weeks after a 2.0mm ear punch under various cecal**

535 **transplantation conditions**

Primary microbiome transplantation					
Mouse group	**N**	**Earhole closure (mm)**	**Earhole closure P values vs. (sex-matched) B6-vehicle**	**Earhole closure P values vs. (sex matched) MRL-vehicle**	**Earhole closure P values, male vs. female**
B6-vehicle	**25**	**0.25±0.03**		**6.9E-10**	**0.059**
Females	12	0.31±0.04		1.7E-10	
Males	13	0.19±0.04		1.5E-12	
MRL-transplanted B6	**36**	**0.74±0.05**	**6.9E-10**	**1.8E-12**	**0.096**
Females	18	0.82±0.09	1.8E-7	2.5E-7	
Males	18	0.65±0.05	8.0E-5	1.8E-7	
B6-transplanted MRL	**21**	**1.28±0.10**		**0.20**	**1.6E-6**
Females	8	1.77±0.06		0.13	
Males	13	0.99±0.08		0.025	
MRL-vehicle	**28**	**1.40±0.07**	**6.9E-10**		**0.0031**
Females	15	1.49±0.10	4.0E-13		
Males	13	1.30±0.08	2.4E-12		
Heritability: earhole closure results of MRL-transplanted B6 mouse offspring					

Mouse group	N	Earhole closure (mm)	Earhole closure P values vs.(sex-matched) B6-vehicle	Earhole closure P values vs.(sex matched) primary MRL-transplanted B6	Earhole closure P values, male vs. female
Offspring of MRL-transplanted B6	**39**	**0.63±0.03**	**4.6E-11**	**0.092**	**0.0038**
Sire + Dam transplanted	4	0.65±0.02	1.8E-5	0.71	
Dam only transplanted	23	0.65±0.04	1.1E-8	0.25	
Sire only transplanted	12	0.60±0.07	5.1E-6	0.16	
Female offspring	20	0.73±0.04	6.4E-7	0.35	
Male offspring	19	0.54±0.05	1.5E-6	0.10	

538 **Table 2: Top imputed microbiome metagenomes correlated with earhole closure rates**

539 **among B6-vehicle, MRL-transplanted B6, and MRL-vehicle mouse groups.**

540

KEGG pathway correlated with earhole closure	Pearson R value	*P* value of correlation
Beta-Lactam resistance	-0.78	0.003
Penicillin and cephalosporin biosynthesis	-0.78	6E-4
1,1,1-Trichloro-2,2-bis(4-chlorophenyl)ethane (DDT) degradation	-0.77	0.008
Glycosphingolipid biosynthesis - ganglio series	-0.75	6E-4
Lipopolysaccharide biosynthesis	-0.73	5E-4
Meiosis - yeast	-0.73	4E-4
Fatty acid elongation in mitochondria	-0.73	4E-4
Proximal tubule bicarbonate reclamation	-0.73	3E-4
Caffeine metabolism	-0.73	4E-4
Fluorobenzoate degradation	-0.73	4E-4
Circadian rhythm - plant	-0.73	4E-4
Steroid biosynthesis	-0.73	4E-4

Ubiquitin system	-0.72	5E-4
Primary immunodeficiency	0.56	0.004
Basal transcription factors	0.61	0.004
Mineral absorption	0.66	0.003
Flavone and flavonol biosynthesis	0.72	0.005
D-Arginine and D-ornithine metabolism	0.73	0.006

543 **Figure Legends:**

544 **Figure 1:** Mouse earhole closure results 4 weeks after a 2.0mm ear punch under various
545 microbiome conditions. **(A)** Earhole closure in transplanted mice at weaning. Line represents
546 mean, whiskers represent SEM. **(B)** Earhole closure in MRL-transplanted B6 mice, where
547 transplantation occurred at various times relative to earhole punch. **(C)** Comparison of earhole
548 closure in MRL-transplanted B6 mice, where transplants were performed at weaning (3-4 weeks
549 of age) vs. as adults (12 weeks of age). **(D)** Differences in earhole closure rates in mice (donors
550 and recipients) raised in-house compared to those purchased from a commercial vendor
551 (Jackson laboratories) and immediately used. **(E)** Earhole closure of MRL-transplanted B6 mice
552 compared to offspring of MRL-transplanted B6 mice.
553
554 **Figure 2:** 16S deep sequencing analysis of cecal samples. **(A)** Alpha diversity by observed
555 OUT method following rarefaction of transplantation mouse groups. Dot represents mean, lines
556 represent SEM. **(B)** Beta diversity plot by weighted unifrac method of mouse 16S samples by
557 group. **(C)** Statistically significant differences in cecal microbiome composition in various mouse
558 groups. Bars represent linear discriminant analysis (LDA) effect size scores. **(D)** Plots of cecal
559 clades most strongly correlated with individual earhole closure rates. B6-vehicle, MRL-vehicle,
560 MRL-transplanted B6, and progeny of MRL-transplanted B6 mice included. **(E)** Cecal
561 microbiome Gram negative proportion data, including dot plot (line represents mean, whiskers
562 represent SEM) and linear correlation. B6-vehicle, MRL-vehicle, MRL-transplanted B6, and
563 progeny of MRL-transplanted B6 mice included.
564
565 **Figure 3**: Disparities in mouse earhole closure and cecal microbiome analysis by mouse sex.
566 **(A)** Earhole closure results separated by sex, lines represent mean, whiskers represent SEM.
567 **(B)** Beta diversity plot of mice by weighted unifrac method, colors represent mouse sex. **(C)**
568 Statistically significant differences in cecal microbiome composition by sex. Bars represent
569 linear discriminant analysis (LDA) effect size scores.

570
571 **References:**

572

573

574 1. Murphy ED, Roths JB. Autoimmunity and lymphoproliferation: induction by mutant gene lpr,
575 and acceleration by a male-associated factor in strain BXSB mice. 1978; 207.

576 2. Adachi M, Watanabe-Fukunaga R, Nagata S. Aberrant transcription caused by the insertion
577 of an early transposable element in an intron of the Fas antigen gene of lpr mice. Proc Natl
578 Acad Sci U S A. 1993;90: 1756–1760.

579 3. Clark LD, Clark RK, Heber-Katz E. A new murine model for mammalian wound repair and
580 regeneration. Clin Immunol Immunopathol. 1998;88: 35–45.

581 4. Heber-Katz E. The regenerating mouse ear. Semin Cell Dev Biol. 1999;10: 415–419.

582 5. Chadwick RB, Bu L, Yu H, Hu Y, Wergedal JE, Mohan S, et al. Digit tip regrowth and
583 differential gene expression in MRL/Mpj, DBA/2, and C57BL/6 mice. Wound Repair Regen.
584 2007;15: 275–284.

585 6. Han M, Yang X, Taylor G, Burdsal CA, Anderson RA, Muneoka K. Limb regeneration in
586 higher vertebrates: developing a roadmap. Anat Rec B New Anat. 2005;287: 14–24.

587 7. Buckley G, Metcalfe AD, Ferguson MWJ. Peripheral nerve regeneration in the MRL/MpJ
588 ear wound model. J Anat. 2011;218: 163–172.

589 8. Leferovich JM, Bedelbaeva K, Samulewicz S, Zhang XM, Zwas D, Lankford EB, et al. Heart
590 regeneration in adult MRL mice. Proc Natl Acad Sci U S A. 2001;98: 9830–9835.

591 9. Naseem RH, Meeson AP, Michael Dimaio J, White MD, Kallhoff J, Humphries C, et al.
592 Reparative myocardial mechanisms in adult C57BL/6 and MRL mice following injury.
593 Physiol Genomics. 2007;30: 44–52.

594 10. Hrbek T, de Brito RA, Wang B, Pletscher LS, Cheverud JM. Genetic characterization of a
595 new set of recombinant inbred lines (LGXSM) formed from the intercross of SM/J and LG/J
596 inbred mouse strains. Mamm Genome. 2006;17: 417.

597 11. Rai MF, Hashimoto S, Johnson EE, Janiszak KL, Fitzgerald J, Heber-Katz E, et al.
598 Heritability of articular cartilage regeneration and its association with ear wound healing in
599 mice. Arthritis Rheum. 2012;64: 2300–2310.

600 12. Rai MF, Sandell LJ. Regeneration of articular cartilage in healer and non-healer mice.
601 Matrix Biol. 2014;39: 50–55.

602 13. Li X, Gu W, Masinde G, Hamilton-Ulland M, Xu S, Mohan S, et al. Genetic control of the
603 rate of wound healing in mice. Heredity . 2001;86: 668–674.

604 14. Blankenhorn EP, Bryan G, Kossenkov AV, Clark LD, Zhang X-M, Chang C, et al. Genetic

605 loci that regulate healing and regeneration in LG/J and SM/J mice. Mamm Genome.
606 2009;20: 720–733.

607 15. Masinde G, Li X, Baylink DJ, Nguyen B, Mohan S. Isolation of wound healing/regeneration
608 genes using restrictive fragment differential display-PCR in MRL/MPJ and C57BL/6 mice.
609 Biochem Biophys Res Commun. 2005;330: 117–122.

610 16. Rai MF, Schmidt EJ, McAlinden A, Cheverud JM, Sandell LJ. Molecular insight into the
611 association between cartilage regeneration and ear wound healing in genetic mouse
612 models: targeting new genes in regeneration. G3 . 2013;3: 1881–1891.

613 17. Gurtner GC, Werner S, Barrandon Y, Longaker MT. Wound repair and regeneration.
614 Nature. 2008. pp. 314–321. doi:10.1038/nature07039

615 18. Leonard CA, Lee W-Y, Tailor P, Salo PT, Kubes P, Krawetz RJ. Allogeneic Bone Marrow
616 Transplant from MRL/MpJ Super-Healer Mice Does Not Improve Articular Cartilage Repair
617 in the C57Bl/6 Strain. PLoS One. 2015;10: e0131661.

618 19. Chinzei N, Rai MF, Hashimoto S, Schmidt EJ, Takebe K, Cheverud JM, et al. Evidence for
619 Genetic Contribution to Variation in Posttraumatic Osteoarthritis in Mice. Arthritis &
620 Rheumatology. 2019;71: 370–381.

621 20. Fitzgerald J, Rich C, Burkhardt D, Allen J, Herzka AS, Little CB. Evidence for articular
622 cartilage regeneration in MRL/MpJ mice. Osteoarthritis Cartilage. 2008;16: 1319–1326.

623 21. Sharma A, Kudesia P, Shi Q, Gandhi R. Anxiety and depression in patients with
624 osteoarthritis: impact and management challenges. Open Access Rheumatol. 2016;8: 103–
625 113.

626 22. Swain S, Sarmanova A, Coupland C, Doherty M, Zhang W. Comorbidities in Osteoarthritis:
627 A systematic review and meta-analysis of observational studies. Arthritis Care Res . 2019.
628 Available: https://onlinelibrary.wiley.com/doi/abs/10.1002/acr.24008

629 23. Wang H, Bai J, He B, Hu X, Liu D. Osteoarthritis and the risk of cardiovascular disease: a
630 meta-analysis of observational studies. Sci Rep. 2016;6: 39672.

631 24. Centers for Disease Control and Prevention (CDC). Prevalence of doctor-diagnosed
632 arthritis and arthritis-attributable activity limitation--United States, 2010-2012. MMWR Morb
633 Mortal Wkly Rep. 2013;62: 869–873.

634 25. Lleal M, Sarrabayrouse G, Willamil J, Santiago A, Pozuelo M, Manichanh C. A single faecal
635 microbiota transplantation modulates the microbiome and improves clinical manifestations
636 in a rat model of colitis. EBioMedicine. 2019. doi:10.1016/j.ebiom.2019.10.002

637 26. Manichanh C, Reeder J, Gibert P, Varela E, Llopis M, Antolin M, et al. Reshaping the gut
638 microbiome with bacterial transplantation and antibiotic intake. Genome Res. 2010;20:
639 1411–1419.

640 27. 16S Sample Preparation Guide. Available:
641 https://support.illumina.com/documents/documentation/chemistry_documentation/16s/16s-
642 metagenomic-library-prep-guide-15044223-b.pdf

643 28. Caporaso JG, Kuczynski J, Stombaugh J, Bittinger K, Bushman FD, Costello EK, et al.

644 QIIME allows analysis of high-throughput community sequencing data. Nat Methods.
645 2010;7: 335–336.

646 29. Edgar RC. Search and clustering orders of magnitude faster than BLAST. Bioinformatics.
647 2010;26: 2460–2461.

648 30. McDonald D, Price MN, Goodrich J, Nawrocki EP, DeSantis TZ, Probst A, et al. An
649 improved Greengenes taxonomy with explicit ranks for ecological and evolutionary
650 analyses of bacteria and archaea. ISME J. 2012;6: 610–618.

651 31. Chang Q, Luan Y, Sun F. Variance adjusted weighted UniFrac: a powerful beta diversity
652 measure for comparing communities based on phylogeny. BMC Bioinformatics. 2011;12:
653 118.

654 32. Hamady M, Knight R. Microbial community profiling for human microbiome projects: Tools,
655 techniques, and challenges. Genome Res. 2009;19: 1141–1152.

656 33. Segata N, Izard J, Waldron L, Gevers D, Miropolsky L, Garrett WS, et al. Metagenomic
657 biomarker discovery and explanation. Genome Biol. 2011;12: R60.

658 34. Kruskal WH, Wallis WA. Use of Ranks in One-Criterion Variance Analysis. J Am Stat
659 Assoc. 1952;47: 583–621.

660 35. Fisher RA. THE USE OF MULTIPLE MEASUREMENTS IN TAXONOMIC PROBLEMS.
661 Ann Eugen. 1936;7: 179–188.

662 36. Battaglia T. LEfSe · An Introduction to QIIME 1.9.1. [cited 14 Feb 2018]. Available:
663 https://twbattaglia.gitbooks.io/introduction-to-qiime/content/lefse.html

664 37. Langille MGI, Zaneveld J, Caporaso JG, McDonald D, Knights D, Reyes JA, et al.
665 Predictive functional profiling of microbial communities using 16S rRNA marker gene
666 sequences. Nat Biotechnol. 2013;31: 814–821.

667 38. Kanehisa M, Goto S. KEGG: kyoto encyclopedia of genes and genomes. Nucleic Acids
668 Res. 2000;28: 27–30.

669 39. Parks DH, Tyson GW, Hugenholtz P, Beiko RG. STAMP: statistical analysis of taxonomic
670 and functional profiles. Bioinformatics. 2014;30: 3123–3124.

671 40. Le Roy T, Debédat J, Marquet F, Da-Cunha C, Ichou F, Guerre-Millo M, et al. Comparative
672 Evaluation of Microbiota Engraftment Following Fecal Microbiota Transfer in Mice Models:
673 Age, Kinetic and Microbial Status Matter. Front Microbiol. 2018;9: 3289.

674 41. Rasmussen TS, de Vries L, Kot W, Hansen LH, Castro-Mejía JL, Vogensen FK, et al.
675 Mouse Vendor Influence on the Bacterial and Viral Gut Composition Exceeds the Effect of
676 Diet. Viruses. 2019;11. doi:10.3390/v11050435

677 42. Ericsson AC, Davis JW, Spollen W, Bivens N, Givan S, Hagan CE, et al. Effects of vendor
678 and genetic background on the composition of the fecal microbiota of inbred mice. PLoS
679 One. 2015;10: e0116704.

680 43. Ma H-L, Blanchet TJ, Peluso D, Hopkins B, Morris EA, Glasson SS. Osteoarthritis severity
681 is sex dependent in a surgical mouse model. Osteoarthritis Cartilage. 2007;15: 695–700.

682 44. Huang H, Skelly JD, Ayers DC, Song J. Age-dependent Changes in the Articular Cartilage
683 and Subchondral Bone of C57BL/6 Mice after Surgical Destabilization of Medial Meniscus.
684 Sci Rep. 2017;7: 42294.

685 45. Peng C, Xu X, Li Y, Li X, Yang X, Chen H, et al. Sex-specific association between the gut
686 microbiome and high-fat diet-induced metabolic disorders in mice. Biol Sex Differ. 2020;11:
687 5.

688 46. Min Y, Ma X, Sankaran K, Ru Y, Chen L, Baiocchi M, et al. Sex-specific association
689 between gut microbiome and fat distribution. Nature Communications. 2019.
690 doi:10.1038/s41467-019-10440-5

691 47. Wang J, Lang T, Shen J, Dai J, Tian L, Wang X. Core Gut Bacteria Analysis of Healthy
692 Mice. Front Microbiol. 2019;10: 887.

693 48. Boer CG, Radjabzadeh D, Medina-Gomez C, Garmaeva S, Schiphof D, Arp P, et al.
694 Intestinal microbiome composition and its relation to joint pain and inflammation. Nat
695 Commun. 2019;10: 4881.

696 49. Langille MG, Meehan CJ, Koenig JE, Dhanani AS, Rose RA, Howlett SE, et al. Microbial
697 shifts in the aging mouse gut. Microbiome. 2014;2: 50.

698 50. Dunn CM, Velasco C, Rivas A, Andrews M, Garman C, Jacob PB, et al. Identification of
699 cartilage microbial DNA signatures and associations with knee and hip osteoarthritis.
700 Arthritis Rheumatol. 2020. doi:10.1002/art.41210

701 51. Rios JL, Bomhof MR, Reimer RA, Hart DA, Collins KH, Herzog W. Protective effect of
702 prebiotic and exercise intervention on knee health in a rat model of diet-induced obesity.
703 Sci Rep. 2019;9: 3893.

704 52. Soderborg TK, Clark SE, Mulligan CE, Janssen RC, Babcock L, Ir D, et al. The gut
705 microbiota in infants of obese mothers increases inflammation and susceptibility to NAFLD.
706 Nature Communications. 2018. doi:10.1038/s41467-018-06929-0

707 53. Harasymowicz NS, Choi Y-R, Wu C-L, Iannucci L, Tang R, Guilak F. Intergenerational
708 transmission of diet-induced obesity, metabolic imbalance, and osteoarthritis in mice.
709 Arthritis Rheumatol. 2019. doi:10.1002/art.41147

710 54. Romano KA, Martinez-del Campo A, Kasahara K, Chittim CL, Vivas EI, Amador-Noguez D,
711 et al. Metabolic, epigenetic, and transgenerational effects of gut bacterial choline
712 consumption. Cell Host Microbe. 2017;22: 279-290.e7.

713 55. Marques FZ. Missing heritability of hypertension and our microbiome. Circulation.
714 2018;138: 1381–1383.

715 56. Bilotta AJ, Ma C, Huang X, Yang W, Chen L, Yao S, et al. Microbiota metabolites SCFA
716 promote intestinal epithelial repair and wound healing through promoting epithelial cell
717 production of milk fat globule-EGF factor 8. The Journal of Immunology. 2018;200: 53.17-
718 53.17.

719 57. James GA, Swogger E, Wolcott R, Pulcini ED, Secor P, Sestrich J, et al. Biofilms in chronic
720 wounds. Wound Repair Regen. 2008;16: 37–44.

721 58. Wolcott RD, Hanson JD, Rees EJ, Koenig LD, Phillips CD, Wolcott RA, et al. Analysis of
722 the chronic wound microbiota of 2,963 patients by 16S rDNA pyrosequencing. Wound
723 Repair Regen. 2016;24: 163–174.

724 59. Johnson TR, Gómez BI, McIntyre MK, Dubick MA, Christy RJ, Nicholson SE, et al. The
725 Cutaneous Microbiome and Wounds: New Molecular Targets to Promote Wound Healing.
726 Int J Mol Sci. 2018;19. doi:10.3390/ijms19092699

727 60. Secor PR, James GA, Fleckman P, Olerud JE, McInnerney K, Stewart PS. Staphylococcus
728 aureus Biofilm and Planktonic cultures differentially impact gene expression, mapk
729 phosphorylation, and cytokine production in human keratinocytes. BMC Microbiology. 2011.
730 p. 143. doi:10.1186/1471-2180-11-143

731 61. Gupta A, Kumar R, Pal K, Singh V, Banerjee PK, Sawhney RC. Influence of sea buckthorn
732 (Hippophae rhamnoides L.) flavone on dermal wound healing in rats. Mol Cell Biochem.
733 2006;290: 193–198.

734 62. Ferraz CR, Carvalho TT, Manchope MF, Artero NA, Rasquel-Oliveira FS, Fattori V, et al.
735 Therapeutic Potential of Flavonoids in Pain and Inflammation: Mechanisms of Action, Pre-
736 Clinical and Clinical Data, and Pharmaceutical Development. Molecules. 2020;25.
737 doi:10.3390/molecules25030762

738 63. Shi HP, Fishel RS, Efron DT, Williams JZ, Fishel MH, Barbul A. Effect of supplemental
739 ornithine on wound healing. J Surg Res. 2002;106: 299–302.

740 64. Shi HP, Efron DT, Most D, Tantry US, Barbul A. Supplemental dietary arginine enhances
741 wound healing in normal but not inducible nitric oxide synthase knockout mice. Surgery.
742 2000;128: 374–378.

743 65. Zhang W, Sun G, Likhodii S, Liu M, Aref-Eshghi E, Harper PE, et al. Metabolomic analysis
744 of human plasma reveals that arginine is depleted in knee osteoarthritis patients.
745 Osteoarthritis Cartilage. 2016;24: 827–834.

746 66. Meessen JMTA, Saberi-Hosnijeh F, Bomer N, den Hollander W, van der Bom JG, van
747 Hilten JA, et al. Serum fatty acid chain length associates with prevalent symptomatic end-
748 stage osteoarthritis, independent of BMI. Sci Rep. 2020;10: 15459.

749 67. Suleman L. Extracellular Bacterial Proteases in Chronic Wounds: A Potential Therapeutic
750 Target? Adv Wound Care. 2016;5: 455–463.

751 68. Ward BD, Furman BD, Huebner JL, Kraus VB, Guilak F, Olson SA. Absence of
752 posttraumatic arthritis following intraarticular fracture in the MRL/MpJ mouse. Arthritis
753 Rheum. 2008;58: 744–753.

754 69. Bedelbaeva K, Snyder A, Gourevitch D, Clark L, Zhang X-M, Leferovich J, et al. Lack of
755 p21 expression links cell cycle control and appendage regeneration in mice. Proc Natl Acad
756 Sci U S A. 2010;107: 5845–5850.

Figure 1: Mouse earhole closure results 4 weeks after a 2.0mm ear punch under various microbiome transplantation conditions

A. Earhole closure results, mice transplanted at weaning

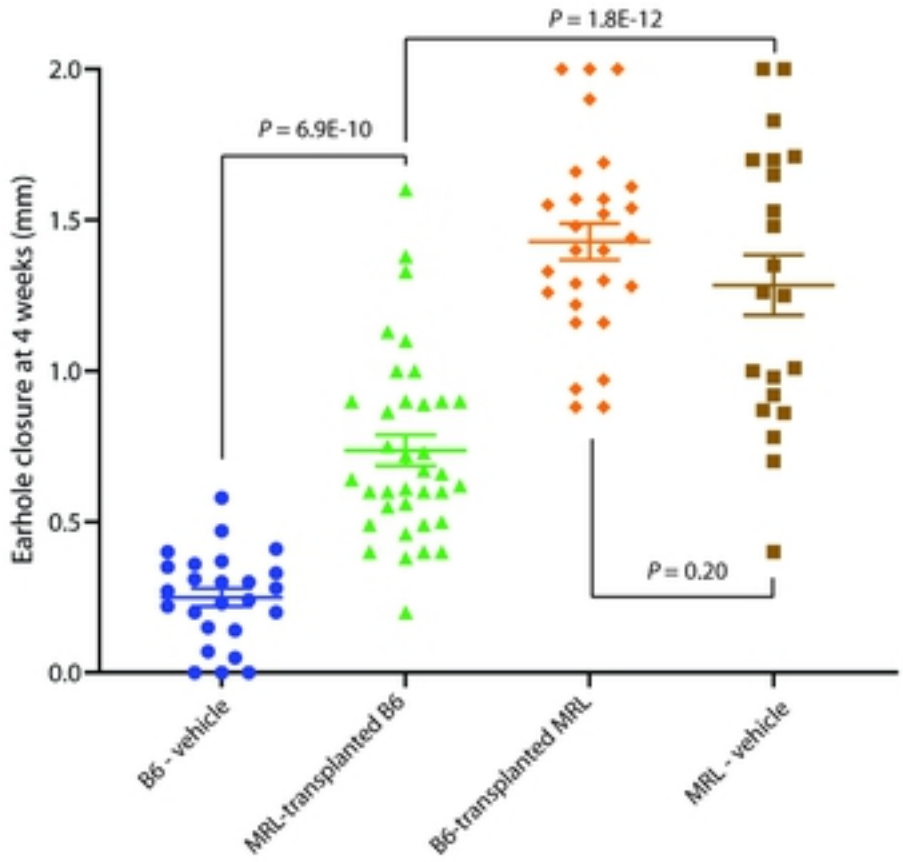

B. Earhole closure results, MRL-transplanted B6 and B6-vehicle, mice transplanted before and after ear punch

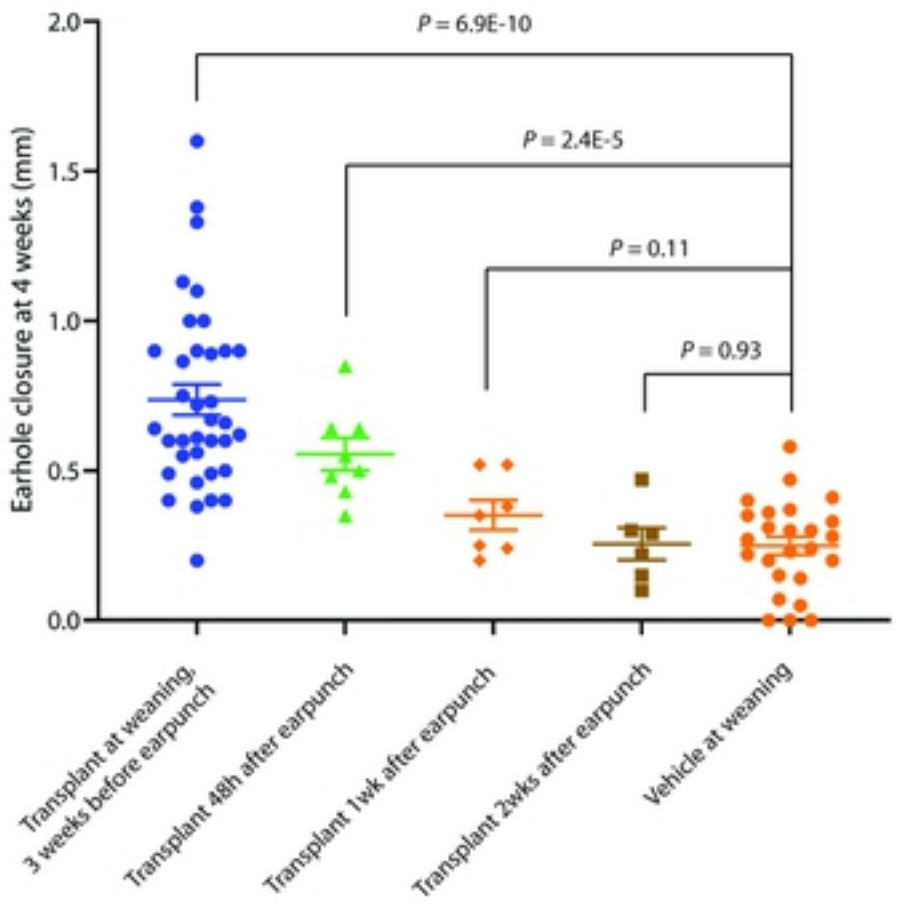

C. Earhole closure results, mice transplanated at weaning vs. as an adult (12-week)

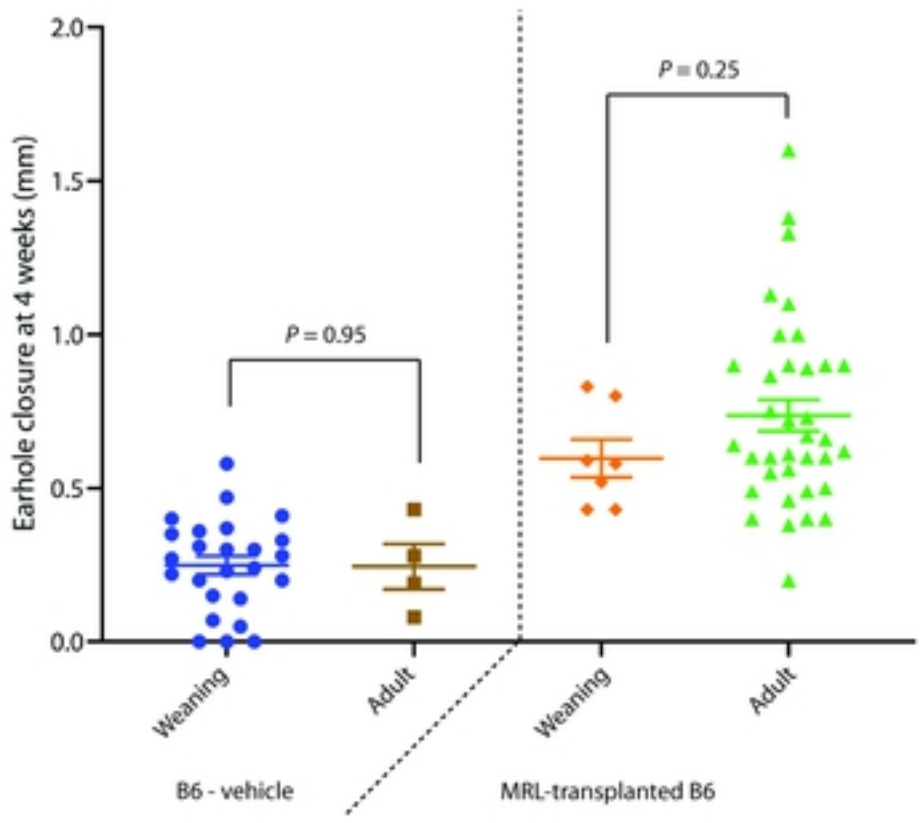

D. Earhole closure differences in mice raised in-house vs. purchased from a commercial vendor, mice transplanted at weaning

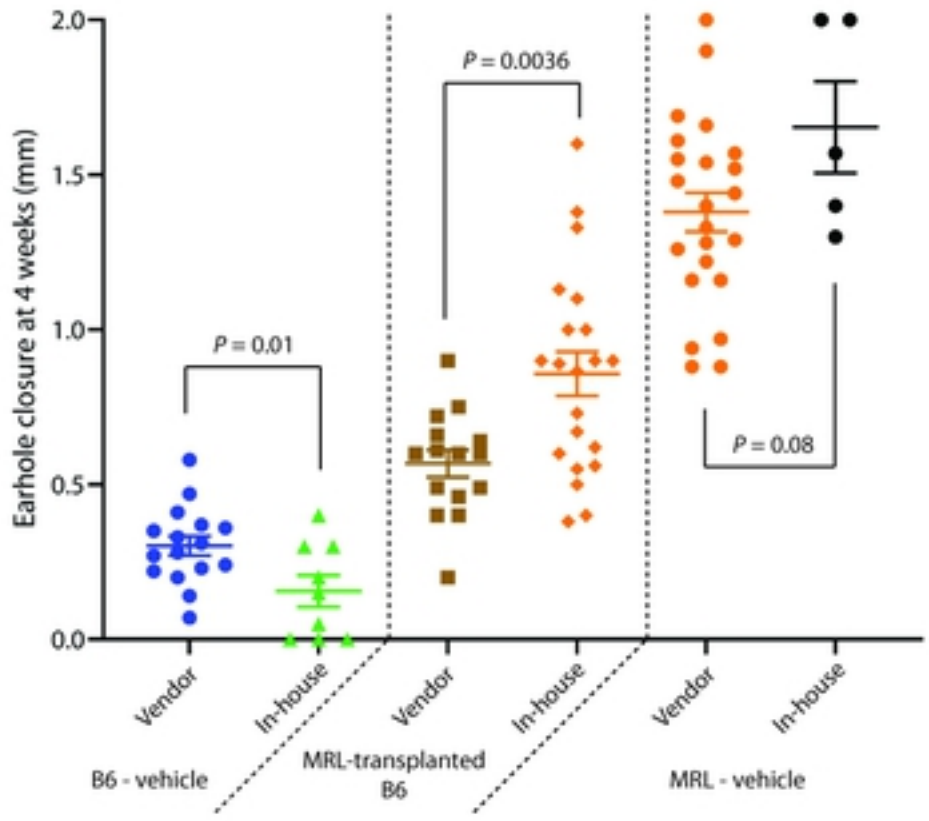

E. Earhole closure results, offspring of MRL-transplanted B6 mice

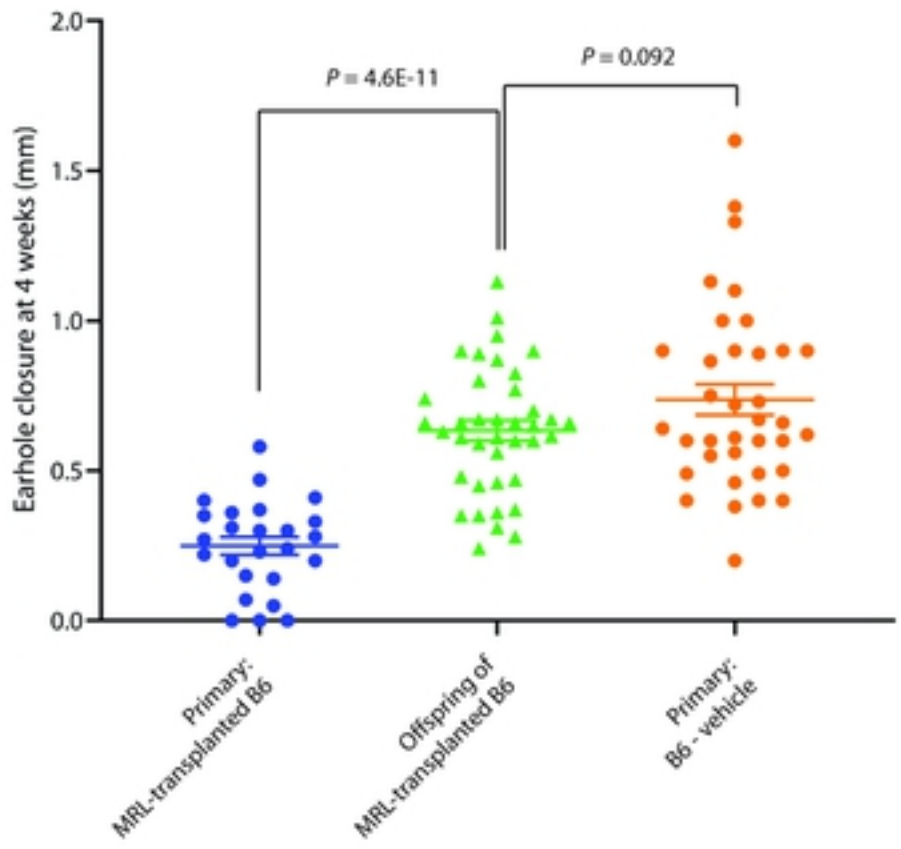

Figure 1

Figure 2: 16S cecal microbiome analysis

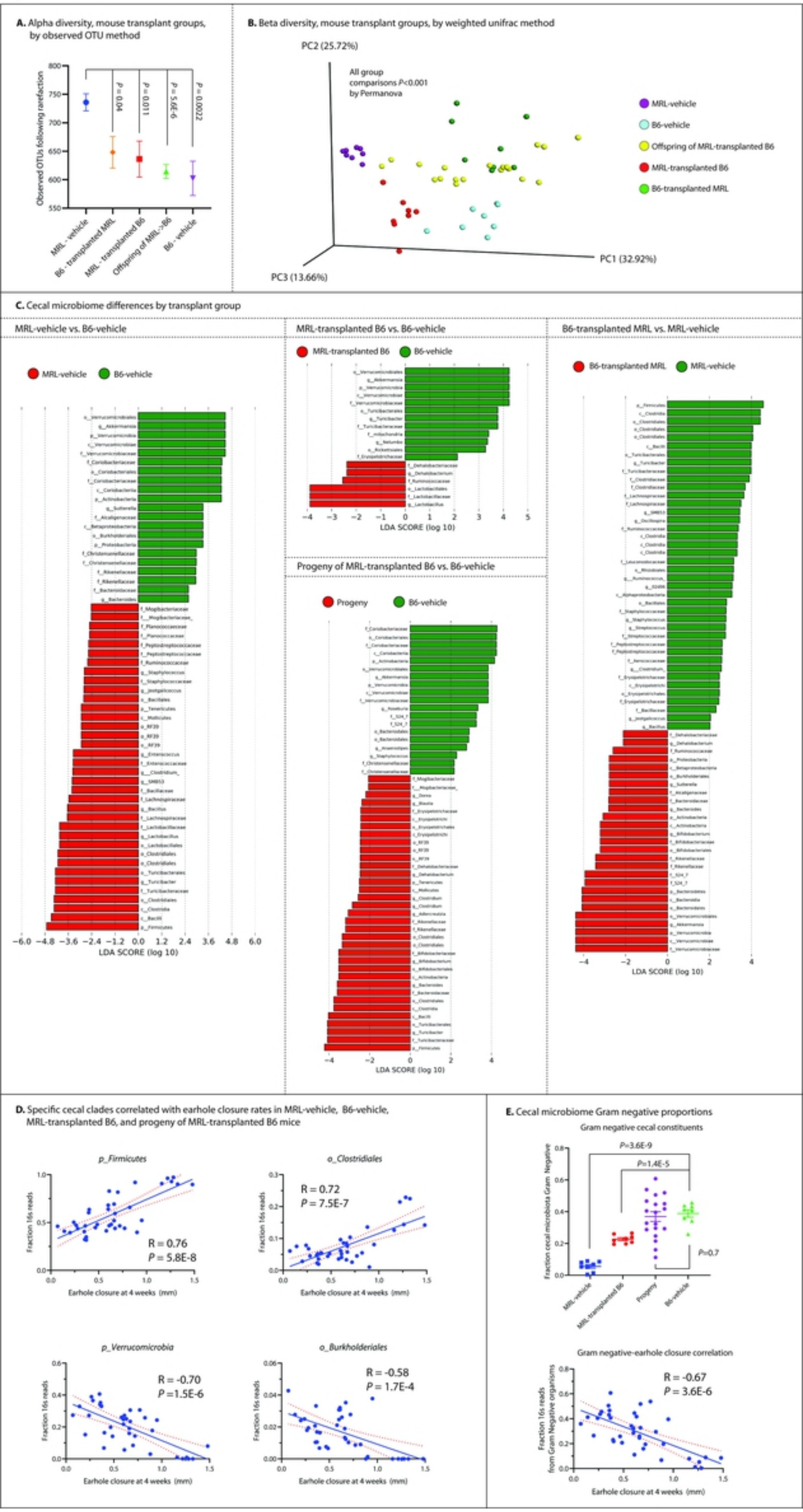

Figure 2

Figure 3: Mouse earhole closure and cecal microbiome analysis 4 weeks after 2.0mm ear punch, separated by mouse sex

A. Earhole closure results, segregated by mouse sex, mice transplanted at weaning

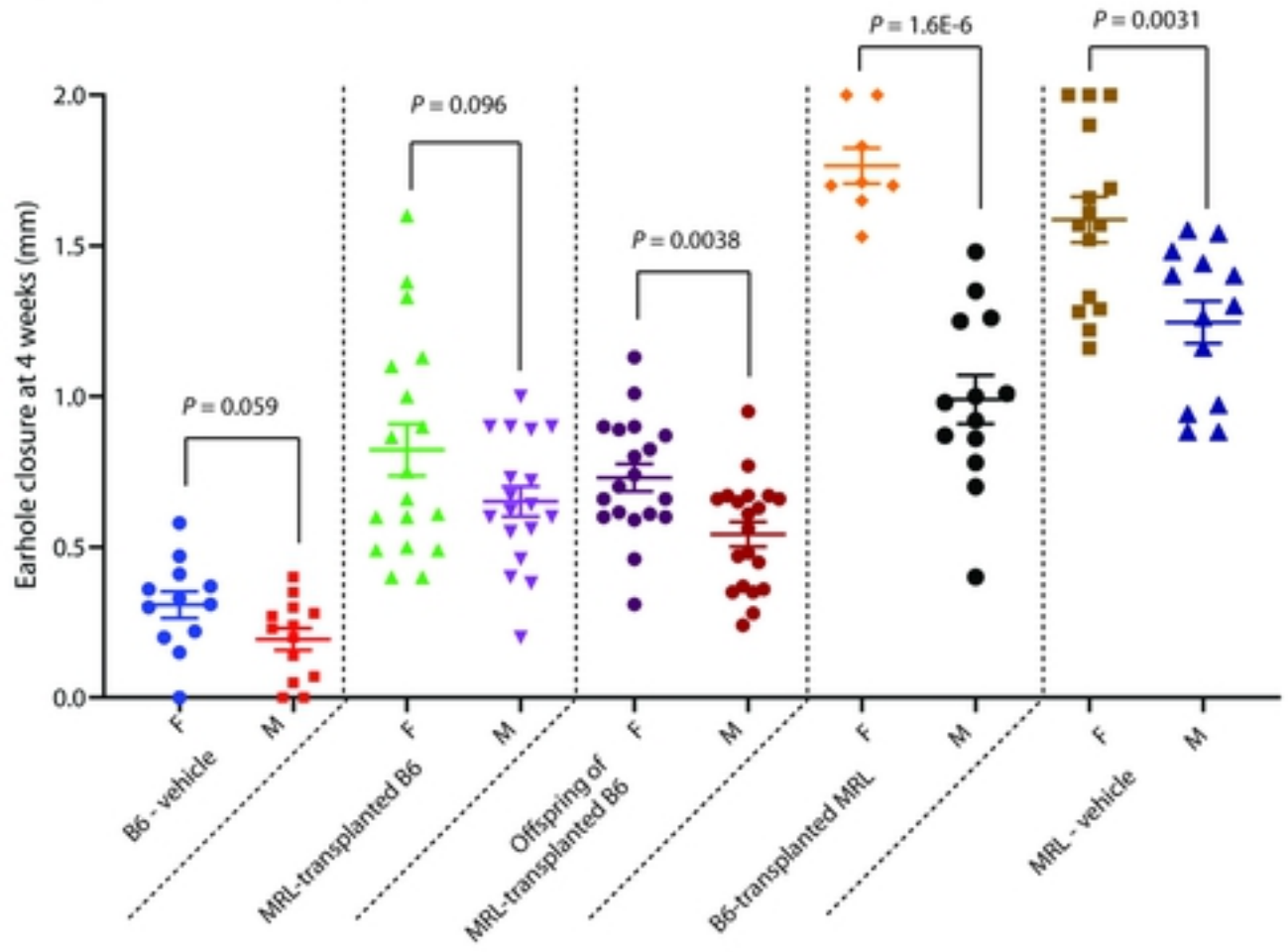

B. Beta diversity, mouse sex, by weighted unifrac method. Mouse transplant groups within dotted ellipses.

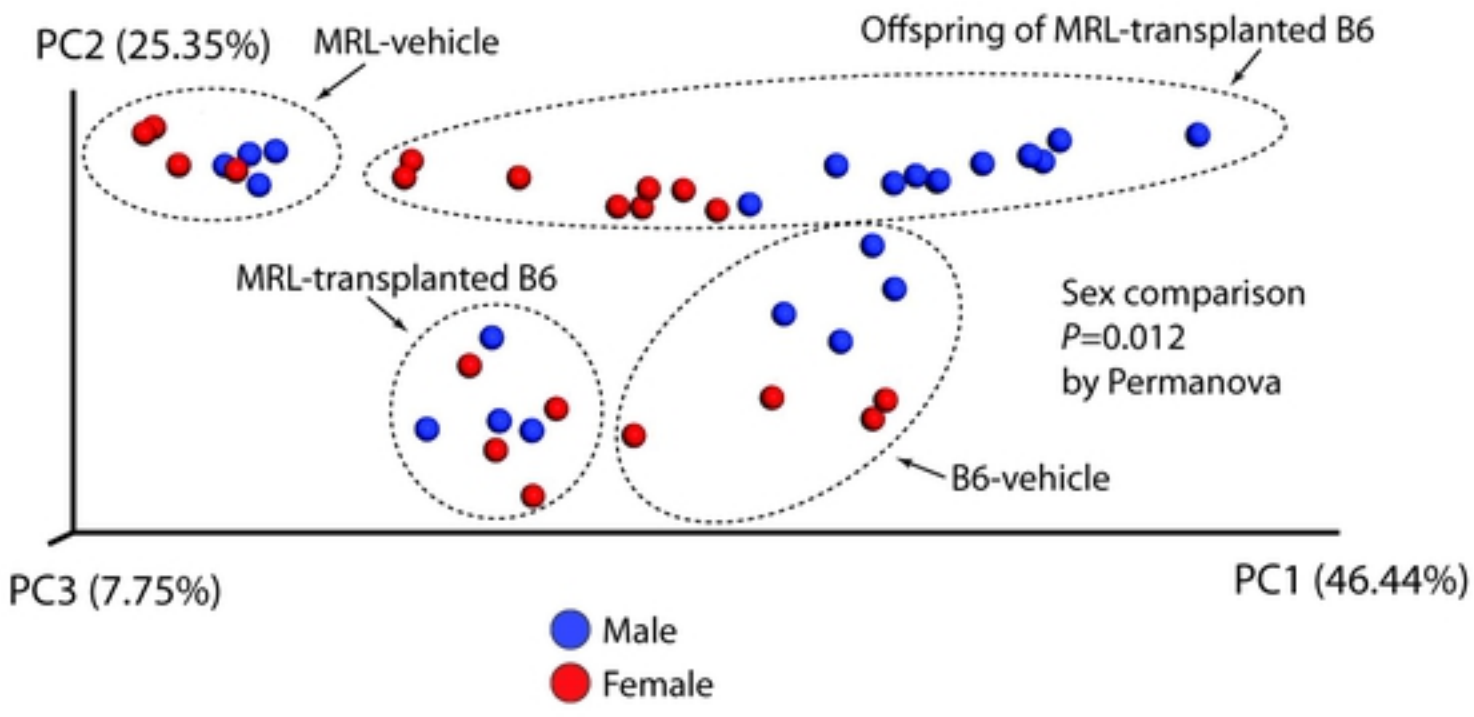

C. Cecal microbiome differences by mouse sex

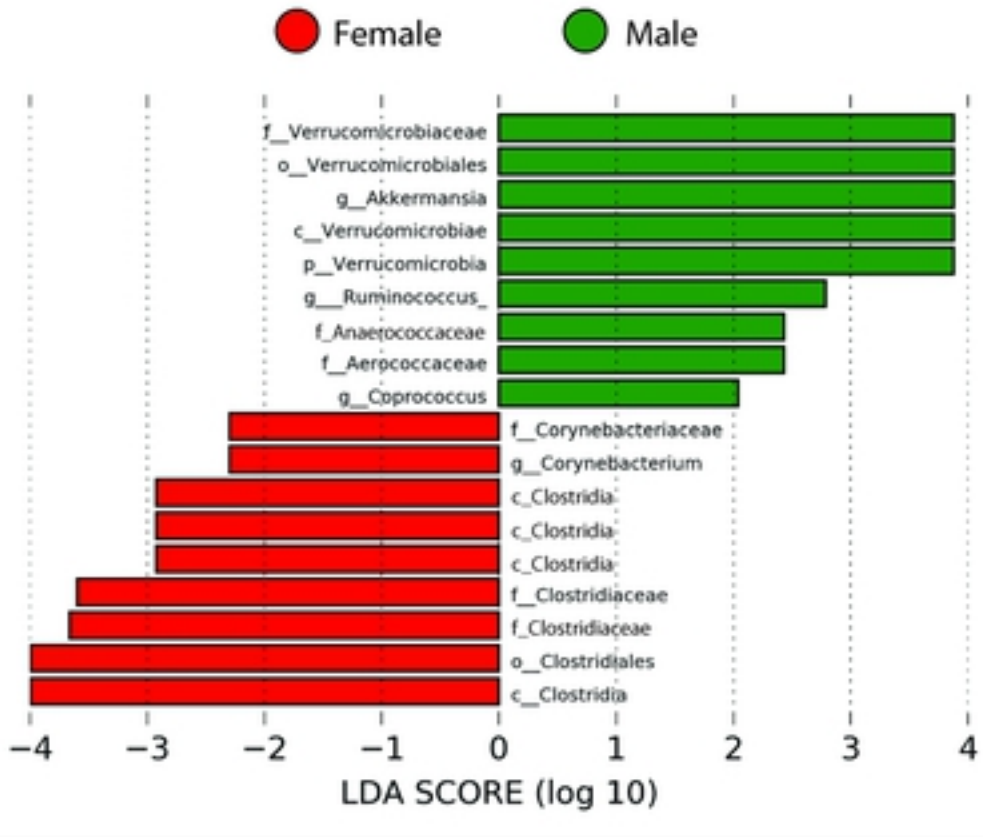

Figure 3